Hindawi
International Journal of Antennas and Propagation
Volume 2019, Article ID 9484836, 8 pages
https://doi.org/10.1155/2019/9484836

Research Article

Heuristic UTD Solution for Antennas Near a Complex Platform

Awika Pimpatang,[1] Titipong Lertwiriyaprapa,[1] and Chuwong Phongcharoenpanich[2]

[1]*Industrial Electric and Control System Research Center, Department of Teacher Training in Electrical Engineering, Faculty of Technical Education, King Mongkut's University of Technology North Bangkok, Bangkok, Thailand*
[2]*Faculty of Engineering, King Mongkut's Institute of Technology Ladkrabang, Bangkok, Thailand*

Correspondence should be addressed to Titipong Lertwiriyaprapa; titipong.l@fte.kmutnb.ac.th

Received 21 June 2018; Revised 8 September 2018; Accepted 6 November 2018; Published 29 January 2019

Academic Editor: Claudio Gennarelli

This paper is aimed at developing an approximate and relatively simple but closed-form uniform geometrical theory of diffraction (UTD) solution for describing the radiated and scattered fields by an antenna near a complex platform consisting of a three-dimensional (3-D) thin material-coated metallic surface, including edges and corners. Unlike the previous works that consider primarily plane wave scattering, the developed solution can also treat radiation/scattering problems of antennas near finite material-coated metallic surfaces which are composed of edges and corners. The developed solution, which is formulated by using a heuristic approach, recovers the proper local plane wave Fresnel reflection coefficient. In addition, the developed UTD-diffracted fields will satisfy the radiation condition, boundary conditions on the conductor. The accuracy of the developed solution is verified by comparing with simulation results from a computer software. It is found that the results from our developed solution agree well with those of references. However, some small discrepancies occur but it is good enough for engineering applications. The proposed solution can be very useful for antenna engineers to design multiple antennas with an electrically large complex material-coated platform.

1. Introduction

In modern antenna system design, platforms are part of the antenna. For example, platforms of modern antenna systems involving modern aircraft, naval ships, or wireless communication system in urban area often contain material treatments over metallic surfaces to control their scattering. It is necessary to include the effects of the platform on the design and development of modern antenna systems. Thus, the efficient and reliable computational tools are needed.

With the advent of large and fast computers, numerical approaches such as the method of moments (MoM), the finite element method (FEM), the finite element boundary integral (FE-BI) method, or the finite different time domain (FDTD) method are able to deal with electromagnetic (EM) radiation/scattering problems at low to moderately high frequencies for which the radiation/scattering platforms are relatively small to moderately large in terms of the EM wavelength, respectively. However, all of these numerical techniques become very poorly convergent, inefficient, and sometimes even intractable at high frequencies. In contrast to the conventional numerical methods mentioned above, the UTD analysis [1] can be performed by identifying all of dominant ray contributions. In order to model the platform accurately, it depends on the availability of the relevant UTD coefficients. Thus, it is necessary to know all the UTD coefficients which are required for predicting the fields of antennas on platforms.

In this paper, the focus is mainly on the UTD analysis of EM diffraction by edges and corners in material-coated PEC planar configuration as shown in Figure 1. The three-dimensional (3-D) skew incidence cases where the source can be a uniform plane wave or a current moment (an antenna) are also of interest here. The material thickness is assumed to be very thin. The material is assumed to be an isotropic and homogeneous material.

Wiener-Hopf (W-H) and Maliuzhinets (MZ) methods are used in the previous works dealing with the analytical solutions for diffraction by canonical material discontinuities [2–4]. These previous works primarily address the scattering

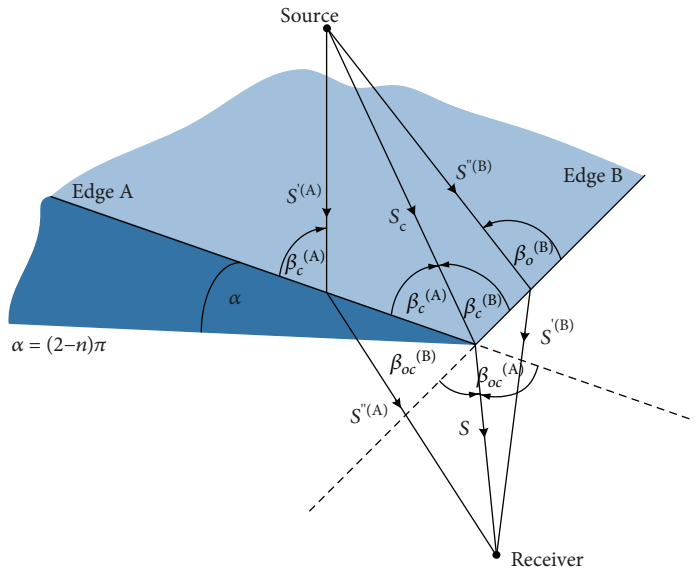

Figure 1: Geometry of PEC wedge configuration including edges and corner.

problem in which the illumination is a uniform plane wave that is an incident on the thin material discontinuity. Among related previous works, which is described in [3], one provides a solution to the problem of the plane wave diffraction by a two-dimensional (2-D) impedance wedge. All of these solutions [2–4] are not relatively simple to use thereby making it unwieldy for engineering applications. In contrast, the works in [5–7] are very useful not only to the analysis of scattering situations but also to antenna problems which are equally important from a practical standpoint. The work in [6, 7] incorporates plane, cylindrical, spherical, and surface wave illumination as well as sources which can be placed directly on a planar material junction on PEC ground plane. This is a 2.5 dimensional (2.5-D) configuration, which has an edge infinitely extended. It is noted that the full 3-D configuration has all dimensions in a finite number. Therefore, in full 3-D configuration, the corner is formed from the composition of two finite edges. Unfortunately, exact analytical solutions to the above problems of wave diffraction are not currently available in a form suitable and tractable for engineering applications.

The UTD work in [1] for a perfectly conducting wedge is heuristically generalized for constructing a UTD solution to describe the diffraction by a material half plane by [8]. The works of [9, 10] are directly extended to study the approximate UTD scattering by a 2-D wedge with impedance boundary conditions. The work in [11, 12] can treat the diffraction by corners of the planar PEC surface. The heuristic works in [13, 14] based on [8] can deal with the non-PEC structure with corners. Recently, the heuristic UTD solution is used for outdoor environment in [15]. The preliminary results of UTD solution for corner and slope diffraction were presented in [16]. It is noted that the major advantages of these heuristic solutions are that they are relatively simple and closed-form expressions which are suitable for engineering applications. Therefore, in this paper, it is of interest to develop a heuristic UTD solution with relatively simple and accurate closed-form expression to deal with the problem of the source (or antenna) placed in the presence of edges and corners in material-coated platforms such as a material-coated PEC square patch and a material-coated PEC square tower platform. It is expected that the proposed solution can be very useful for antenna engineers to design multiple antennas with an electrically large complex material-coated platform.

2. Procedure

The geometry of a corner on a PEC wedge can be shown in Figure 1. The total field $\bar{E}^{\text{tot}}$ for this problem includes incident $\bar{E}^{\text{i}}$, reflected $\bar{E}^{\text{r}}$, edge-diffracted $\bar{E}^{\text{d}}$, and corner-diffracted $\bar{E}^{\text{c}}$ fields which can be written as

$$\bar{E}^{\text{tot}} = \bar{E}^{\text{i}} + \bar{E}^{\text{r}} + \bar{E}^{\text{d}} + \bar{E}^{\text{c}}, \tag{1}$$

where the $\bar{E}^{\text{d}}$ is well known UTD edge-diffracted field [1] which can be written as

$$\bar{E}^{\text{d}} = \bar{\bar{D}}\bar{E}^{\text{i}} \sqrt{\frac{s'}{s\left(s'+s\right)}} e^{-jks}. \tag{2}$$

$\bar{E}^{\text{c}}$ denotes the corner-diffracted field [12] which can be written as

$$\bar{E}^{\text{c}} = \bar{\bar{D}}_c \bar{E}^{\text{i}} \times \frac{e^{-j(\pi/4)}}{\sqrt{2\pi k}} \sqrt{\frac{s'}{s''\left(s'+s''\right)}} \sqrt{\frac{s(s+s_c)}{s_c}} \frac{\sqrt{\sin\beta_c \sin\beta_{0c}}}{(\cos\beta_{0c} - \cos\beta_c)} \times F\left[kL_c a(\pi - \beta_{0c} - \beta_c)\right] \frac{e^{-jks}}{s}. \tag{3}$$

The UTD edge and corner diffraction coefficient are given by

$$\begin{aligned}\overline{\overline{D}} &= \left[AD\left(\phi-\phi'\right)+BD\left(\phi+\phi'\right)\right],\\ \overline{\overline{D}}_c &= \left[AC\left(\phi-\phi'\right)+BC\left(\phi+\phi'\right)\right].\end{aligned} \tag{4}$$

Matrices A and B account for the GO discontinuities at the incident shadow boundary (ISB) and reflection shadow boundary (RSB), respectively. In the case of a PEC wedge, A and B matrices are given by

$$\begin{aligned}A &= \begin{bmatrix}-1 & 0\\ 0 & -1\end{bmatrix},\\ B &= \begin{bmatrix}1 & 0\\ 0 & -1\end{bmatrix}.\end{aligned} \tag{5}$$

$D(x)$ in (2) is given by

$$\begin{aligned}D(x) = \frac{-e^{-j(\pi/4)}}{2n\sqrt{2\pi k}\sin\beta_0}&\left\{\cot\left(\frac{\pi+x}{2n}\right)F\left[kLa^+(x)\right]\right.\\ &\left.+\cot\left(\frac{\pi-x}{2n}\right)F\left[kLa^-(x)\right]\right\},\end{aligned} \tag{6}$$

and $C(x)$ in (4) is given by

$$\begin{aligned}C(x) = \frac{-e^{-j(\pi/4)}}{2n\sqrt{2\pi k}\sin\beta_0}&\left\{\cot\left(\frac{\pi+x}{2n}\right)F\left[kLa^+(x)\right]\right.\\ &\cdot\left|F\left[\frac{\left[\left(La^+(x)\right)/\lambda\right]}{kL_ca(\pi+\beta_{0c}-\beta_c)}\right]\right|+\cot\left(\frac{\pi-x}{2n}\right)F\left[kLa^-\right]\\ &\left.\cdot\left|F\left[\frac{\left[\left(La^-(x)\right)/\lambda\right]}{kL_ca(\pi+\beta_{0c}-\beta_c)}\right]\right|\right\}.\end{aligned} \tag{7}$$

The rest of the parameters in equations (2)–(7) can be found in [13]. To verify the accuracy, it is of interest to use the proposed UTD solution to solve EM diffraction on the edges and corners of a PEC square patch for the case where the corner of square patch n is set to be 2 excited by a half-wavelength dipole antenna as shown in Figure 2. The location of the dipole is h and the width of square patch is w. The radiation pattern at a distance of 100λ for $h=1\lambda$, $w=4\lambda$, and $\phi=20^\circ$ is shown in Figure 3.

From the dashed line of Figure 3, there are two discontinuities, namely, at ISB (around 115°) and at 90°. The first one at ISB (around 115°) occurred because the incident field from a dipole has a rapid spatial variation at the ISB. This discontinuity can be fixed by adding the slope diffraction [17], which can be written as

$$\overline{E}^{\mathrm{ds}} = \frac{1}{jk}\frac{\partial\overline{\overline{D}}}{\partial\phi'}\frac{\partial\overline{E}^{\mathrm{i}}(Q_E)}{\partial n}\sqrt{\frac{s'}{s\left(s'+s\right)}}\frac{e^{-jks}}{s}. \tag{8}$$

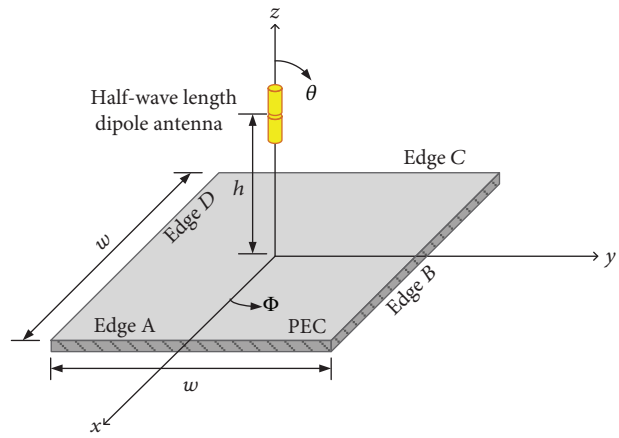

Figure 2: PEC square patch excited by a half-wavelength dipole antenna.

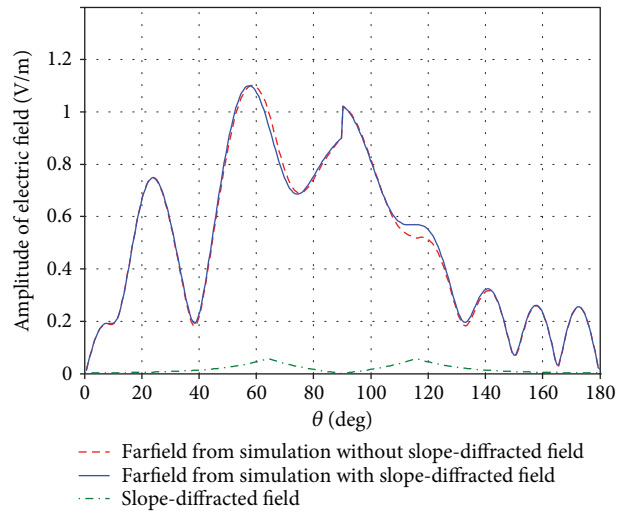

Figure 3: Total field in the $\phi=5^\circ$ plane with $w=4\lambda$ and $h=1\lambda$, at 4 GHz.

The total field with the slope-diffracted field can be shown in the solid line of Figure 3. The slope-diffracted field peeks up at reflection shadow boundary and incident shadow boundary to compensate the rapid spatial variation at both ISB and RSB. Luckily, at RSB, the reflected field is not a rapid variation; thus, there is no discontinuity. However, for the material-coated PEC surface, the slope diffraction can be done via [5].

From Figure 3, it is found that the second discontinuity occurs at 90° and it can be fixed by including the double diffraction as shown in Figure 4, which can be given by

$$\overline{E}^{\mathrm{dd}} = \overline{\overline{D}}\overline{E}^{\mathrm{d}}(Q_1)\sqrt{\frac{s'}{s\left(s'+s\right)}}\frac{e^{-jks}}{s}. \tag{9}$$

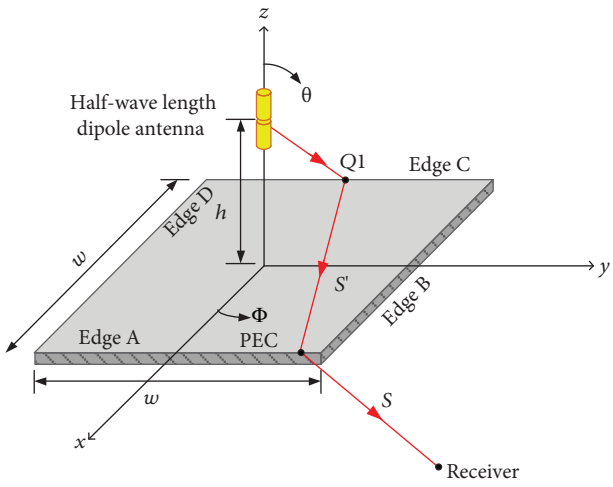

Figure 4: Double diffraction for PEC square patch excited by a half-wavelength dipole antenna.

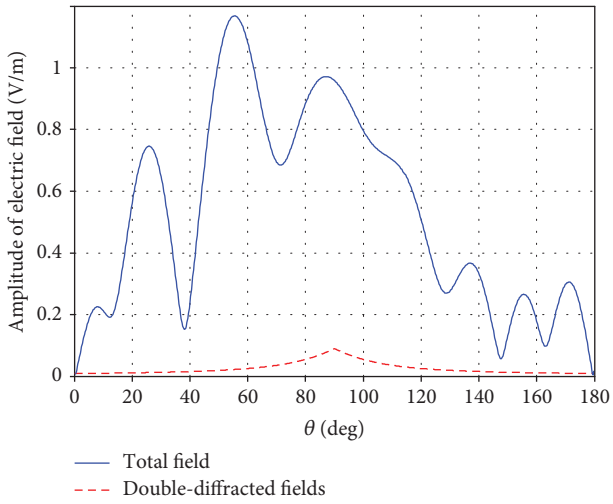

Figure 5: Total field and double-diffracted field in the $\phi = 20^{\circ}$ plane with $w = 4\lambda$ and $h = 1\lambda$, at 4 GHz.

Therefore, the total field can be written as the superposition of incident, reflected, edge-diffracted, corner-diffracted, double-diffracted, and slope-diffracted fields such that

$$\bar{E}^{\text{tot}} = \bar{E}^{\text{i}} + \bar{E}^{\text{r}} + \bar{E}^{\text{d}} + \bar{E}^{\text{c}} + \bar{E}^{\text{dd}} + \bar{E}^{\text{ds}}. \quad (10)$$

The total field from Figure 2 can be shown in Figure 5. It can be observed that the double-diffracted field peaks up at 90° to fix the discontinuous problem. The total field is continuous at 90° as shown in Figure 5.

To verify the accuracy of the UTD solution, the result of a half-wave length dipole antenna above PEC square patches is calculated by using the UTD solution and compared with simulation result from computer software. The amplitude and phase of electric field of the θ component (copolarized) are shown in Figures 6 and 7, respectively. Also, the

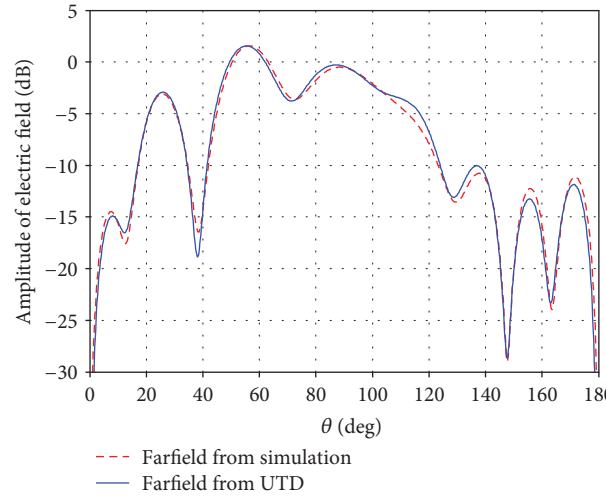

Figure 6: Amplitude of electric field of the θ component in the $\phi = 20^{\circ}$ plane with $w = 4\lambda$ and $h = 1\lambda$, at 4 GHz compared with simulation result.

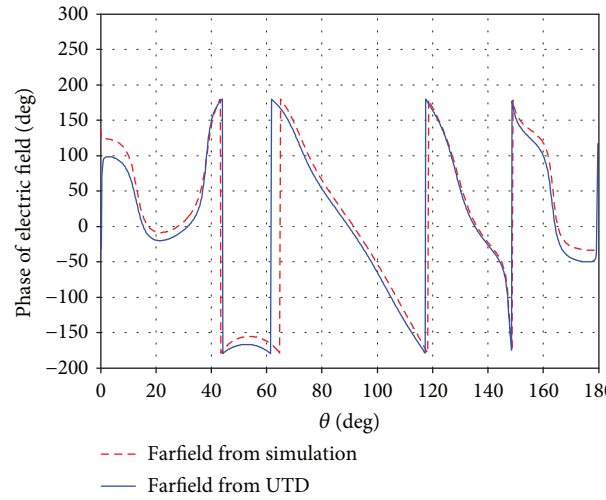

Figure 7: Phase of electric field of the θ component in the $\phi = 20^{\circ}$ plane with $w = 4\lambda$ and $h = 1\lambda$, at 4 GHz compared with simulation result.

amplitude and phase of electric field of the ϕ component (cross-polarized) are shown in Figures 8 and 9, respectively. It is found that the results from the θ component agree well with those from simulation but there are some discrepancies in the ϕ component because the cross-polarized one provides very small field strength (below −20 dB) where the proposed UTD in (10) cannot take into account those small contributions. The higher order term such as triple diffraction is needed.

It is noted that from the result in Figure 9 of [12], the radiation pattern at a distance 64λ for $h = 1\lambda$, $w = 4\lambda$, $\phi = 135^{\circ}$, and $0^{\circ} < \theta < 180^{\circ}$ and discontinuity at grazing $\theta = 90^{\circ}$ can be removed by introducing higher order contributions, like double diffraction rays. In this case, when the

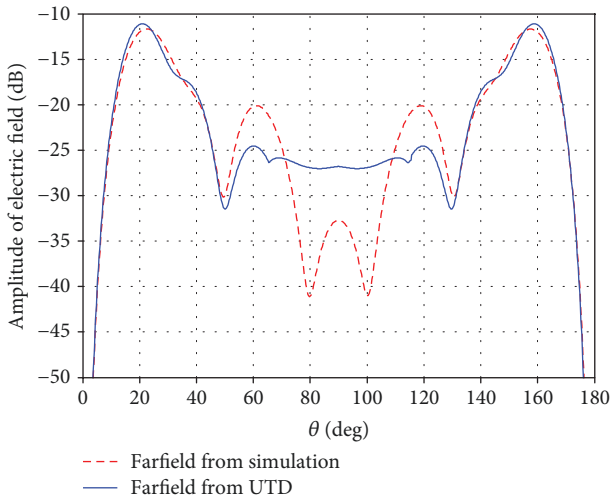

Figure 8: Amplitude of electric field of the ϕ component in the $\phi = 20^{\circ}$plane with $w = 4\lambda$ and $h = 1\lambda$, at 4 GHz compared with simulation result.

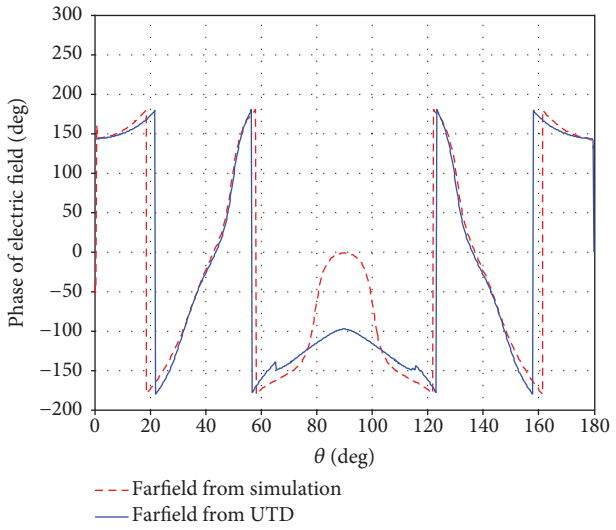

Figure 9: Phase of electric field of the ϕ component in the $\phi = 20^{\circ}$plane with $w = 4\lambda$ and $h = 1\lambda$, at 4 GHz compared with simulation result.

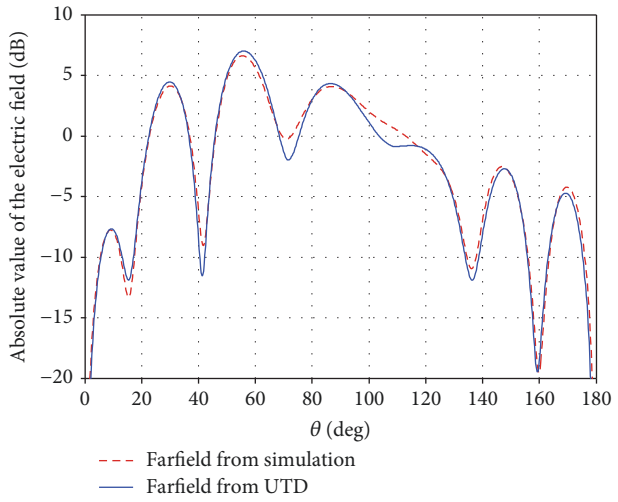

Figure 10: Absolute value of electric field in the $\phi = 45^{\circ}$plane with $w = 4\lambda$ and $h = 1\lambda$, at 4 GHz compared with simulation result.

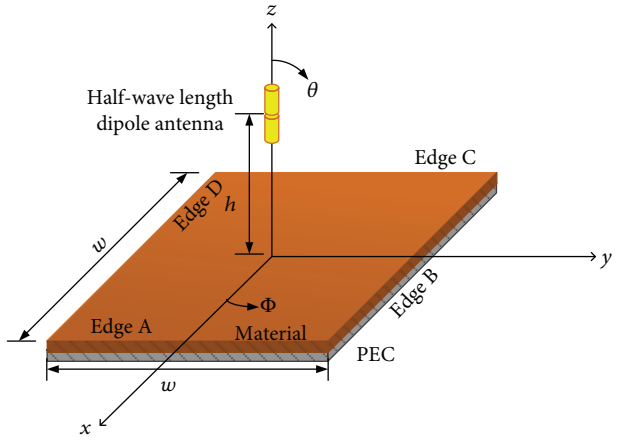

Figure 11: Material-coated PEC square patch excited by a half-wavelength dipole antenna.

double-diffracted field is added, the new total field is continuous at 90° as shown in Figure 10.

In this paper, two examples of a complex platform, excited by a half-wave length dipole, are analyzed, namely, a material-coated PEC square patch and material-coated PEC square tower platform. It is noted that this UTD solution can deal with all kinds of excitations. Thus, the antenna or source is not restricted to the half-wave length dipole antenna. Let us consider the first example of a material-coated PEC square patch excited by a half-wavelength dipole antenna as shown in Figure 11. The material type is FR-4 with $\varepsilon_r = 4.3$, $\mu_r = 1$, thickness $\tau_0 = \lambda/50$, $h = 1\lambda$, and $w = 4\lambda$. The observation distance is 100λ at $\phi = 40^{\circ}$. Equations (1)–(10) for PEC solution can be used by heuristically replacing the A and B matrices by

$$A = \begin{bmatrix} -1 & 0 \\ 0 & -1 \end{bmatrix}, \qquad B = T\left(\phi'\right) R\left(\phi'\right) T\left(\phi'\right), \tag{11}$$

where

$$T\left(\phi'\right) = \begin{bmatrix} \cos\beta_0 \sin\phi' & -\cos\phi' \\ \cos\phi' & \cos\beta_0 \sin\phi' \end{bmatrix}, \qquad R\left(\phi'\right) = \begin{bmatrix} R_M\left(\phi'\right) & 0 \\ 0 & R_E\left(\phi'\right) \end{bmatrix}, \tag{12}$$

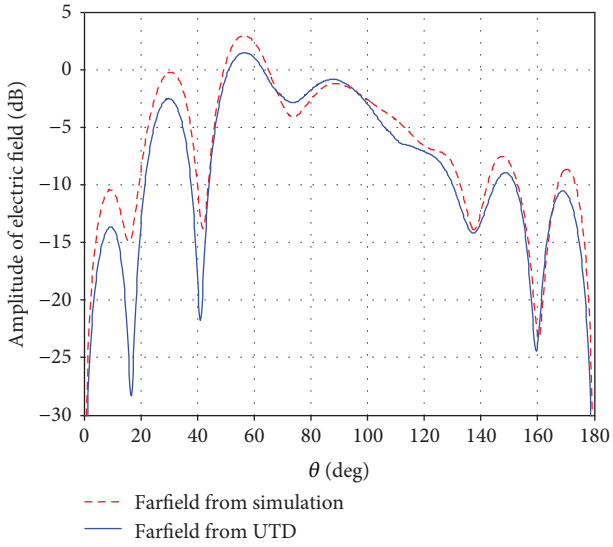

Figure 12: Amplitude of electric field of the θ component in the $\phi = 40^{\circ}$plane with $w = 4\lambda$ and $h = 1\lambda$, at 4 GHz compared with simulation result.

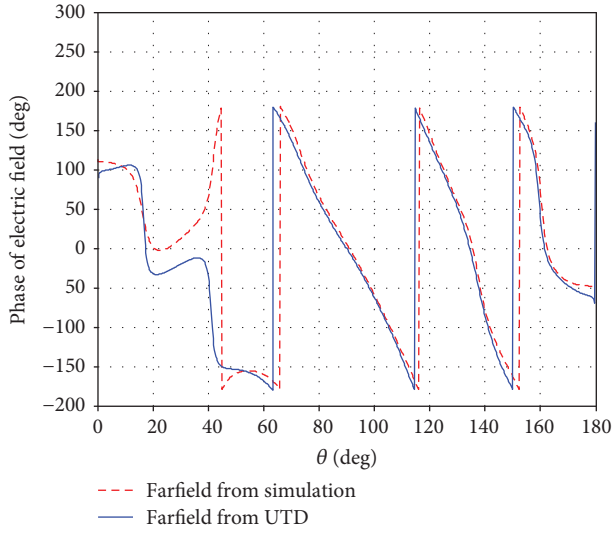

Figure 13: Phase of electric field of the θ component in the $\phi = 40^{\circ}$plane with $w = 4\lambda$ and $h = 1\lambda$, at 4 GHz compared with simulation result.

$$R_{M,E} = \frac{\sin\phi' - \delta_{M,E}/\sin\beta_o}{\sin\phi' + \delta_{M,E}/\sin\beta_o},$$
$$\delta_M = jZ_d N^d \tan\left(k_d N^d \tau_o\right), \tag{13}$$
$$\delta_E = -jY_d N^d \cot\left(k_d N^d \tau_o\right),$$

$$Z_d = \sqrt{\frac{\mu_r}{\varepsilon_r}},$$
$$y_d = \frac{1}{Z_d}, \tag{14}$$
$$k_d = k\sqrt{\mu_r \varepsilon_r},$$
$$N^d = \sqrt{1 - \eta\left(1 - \sin^2\phi' \sin^2\beta_o\right)}, \quad \eta = \frac{1}{\sqrt{\mu_r \varepsilon_r}}.$$

The rest of the parameters in equation (13) can be found in [18].

3. Numerical Results

The radiation patterns from calculation compared with those from simulation consisting of the amplitude and phase of electric field of the θ component (copolarized) are shown in Figures 12 and 13, respectively. Also, the amplitude and phase of electric field of the ϕ component (cross-polarized) are shown in Figures 14 and 15, respectively. The results from the proposed UTD agree well with those from simulation for the θ component (copolarized). However, the results of the ϕ component (cross-polarized) is expected to be very small, which is below −20 dB as shown in Figures 14 and 15. Therefore, there are some discrepancies in the ϕ component (cross-polarized) of Figures 14 and 15 between 60 and 120 degrees due to rounded-off errors from calculation. In addition, there are discontinuities in that region because it is very difficult for the transition function $F[x]$ to compensate the discontinuities which is smaller than −20 dB. This is a limitation of this heuristic solution.

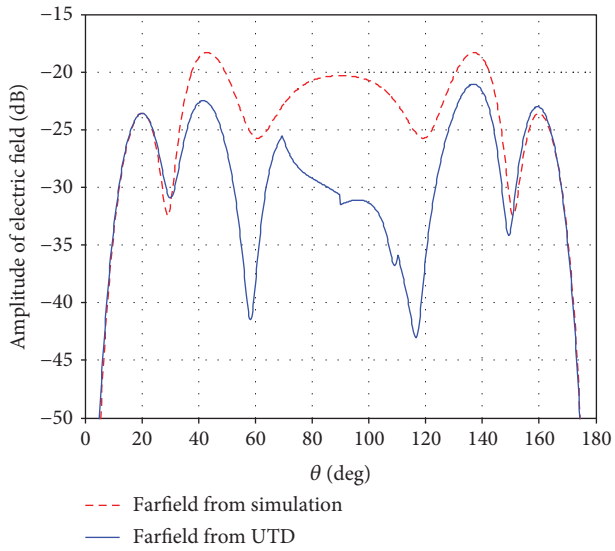

Figure 14: Amplitude of electric field of the ϕ component in the $\phi = 40^{\circ}$plane with $w = 4\lambda$ and $h = 1\lambda$, at 4 GHz compared with simulation result.

Next, let us consider the second example, material-coated PEC square tower platform, excited by a half-wavelength dipole antenna, shown in Figure 16 with $h = 1\lambda$ and $w = 10\lambda$. The observation distance is 1000λ at $\phi = 40^{\circ}$. The platform height is set to be infinite for the UTD solution but the height of the platform is just 100λ in the simulation because it is not possible to model an infinite height of the platform. The radiation patterns from UTD and simulation

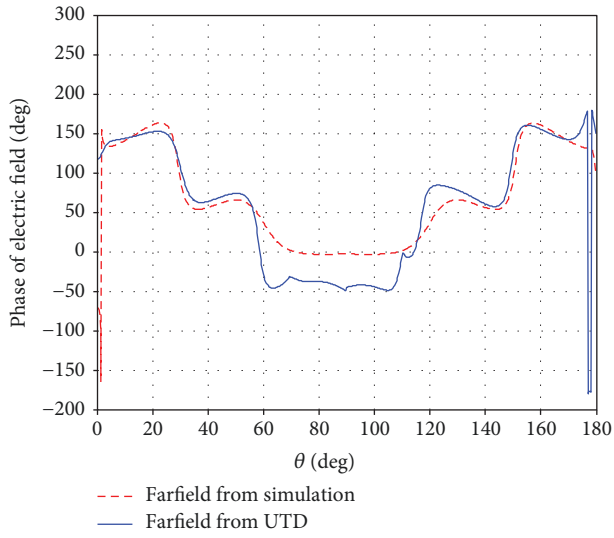

Figure 15: Phase of electric field of the ϕ component in the $\phi = 40^{\circ}$plane with $w = 4\lambda$ and $h = 1\lambda$, at 4 GHz compared with simulation result.

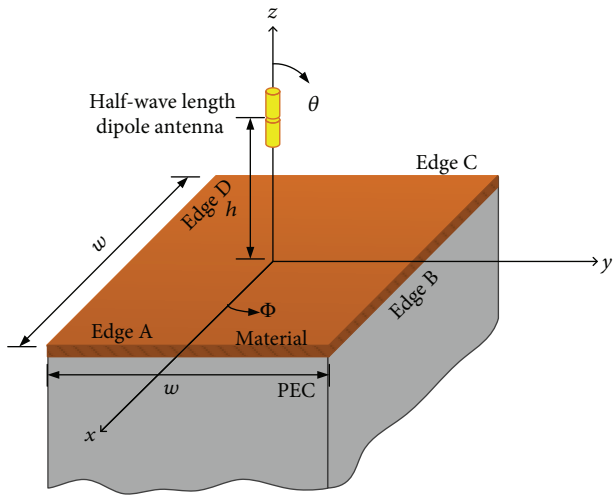

Figure 16: Material-coated PEC square tower platform excited by a simple half-wavelength dipole antenna.

are shown in Figure 17. It is found that the result from UTD agrees well with the simulation result except when the observation angle is beyond 140° due to the effect finite height of the platform, which can occur in the deep shadow region. It can be expected that if the finite height of the platform is taken into account in the UTD solution, the result should agree well with the simulation. The total computational time of simulation was 51 minutes and 4 seconds, but it is only a few seconds for that of the UTD solution. The computer specification is CPU Intel(R) core (TM) i5-6500 3.2 GHz memory (RAM) 16.0 GB.

It is noted that the thickness τ_0 of the material coated in the proposed UTD is assumed to be very thin. Therefore, the thickness of material coated τ_0 equals to $\lambda/50$ or 0.02λ for all of the results above. It is of interest to show the criterion of

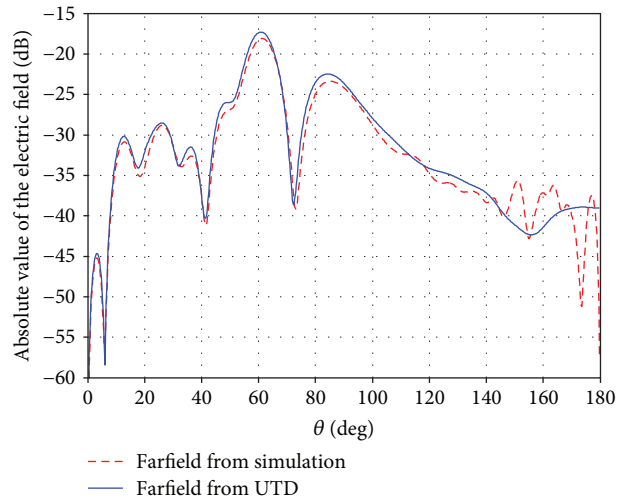

Figure 17: Absolute value of electric field in the $\phi = 40^{\circ}$plane with $w = 10\lambda$ and $h = 1\lambda$, at 4 GHz compared with simulation result.

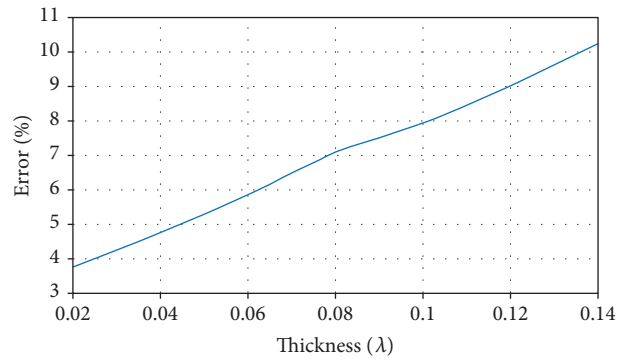

Figure 18: Accuracy of the proposed UTD solution when comparing with the numerical results from simulation versus the variation of thickness of material coated.

the proposed UTD solution regarding the thickness of material coated with variations of thickness by fixing $\phi = 45^{\circ}$, $h = 1\lambda$, $w = 4\lambda$, $\varepsilon_r = 4.3$, and $\mu_r = 1$. The accuracy of the proposed solution is investigated by comparing the numerical results from the proposed UTD solution with the results from simulation via the root mean square error: RMSE as shown in Figure 18.

$$\%\text{RMSE} = \sqrt{\frac{\sum_{i=1}^{N}\left(Z_{f_i} - Z_{O_i}\right)^2}{N}} \times 100, \tag{15}$$

where Z_{f_i} denotes the numerical result from simulation while Z_{O_i} is from the proposed UTD solution. N is the number of data points.

It is found from Figure 18 that the numerical error is increased when the thickness of material coated increased. This plot can be a guideline to use this solution for any

engineering applications. For example, if one prefers the error less than 5%, the thickness should be less than 0.04λ or $\lambda/25$.

4. Conclusion

The closed-form heuristic UTD solution including edge diffraction, corner diffraction, double diffraction, and slope diffraction for antenna problem with a complex platform is proposed in this work. The proposed heuristic UTD solution can be used to solve a finite PEC platform with excitation from an antenna. The accuracy of the UTD is verified by simulation results from computer software. It is found that the proposed UTD solution is easy to use and the accuracy of the developed UTD solution is good enough for engineering application.

Data Availability

The data used to support the findings of this study are available from the corresponding author upon request.

Disclosure

The manuscript is based on a Ph.D. dissertation by Titipong Lertwiriyaprapa (https://etd.ohiolink.edu/!etd.send_file?accession=osu1196281470&disposition=inline), and an earlier version of this work was presented at 2018 Asian Workshop on Antennas and Propagation.

Conflicts of Interest

The authors declare that there is no conflict of interests regarding the publication of this paper.

Acknowledgments

This work is funded by the Thailand Research Fund under Grant no. TRG5680020.

References

[1] R. G. Kouyoumjian and P. H. Pathak, "A uniform geometrical theory of diffraction for an edge in a perfectly conducting surface," *Proceedings of the IEEE*, vol. 62, no. 11, pp. 1448–1461, 1974.

[2] G. D. Maliuzhinets, "Excitation, reflection and emission of surface waves from a wedge with given face impedance," *Soviet Physics - Doklady*, vol. 3, pp. 752–755, 1958.

[3] V. G. Vaccaro, "Electromagnetic diffraction from a right-angled wedge with soft conditions on one face," *Optica Acta: International Journal of Optics*, vol. 28, no. 3, pp. 293–311, 1981.

[4] R. G. Rojas, H. C. Ly, and P. H. Pathak, "Electromagnetic plane wave diffraction by a planar junction of two thin dielectric/ferrite half planes," *Radio Science*, vol. 26, no. 3, pp. 641–660, 1991.

[5] T. Lertwiriyaprapa, P. H. Pathak, and J. L. Volakis, "A UTD for predicting fields of sources near or on thin planar positive/negative material discontinuities," *Radio Science*, vol. 42, article RS6S18, 2007.

[6] T. Lertwiriyaprapa, P. H. Pathak, and J. L. Volakis, "An approximate UTD ray solution for the radiation and scattering by antennas near a junction between two different thin planar material slab on ground plane," *Progress in Electromagnetics Research*, vol. 102, pp. 227–248, 2010.

[7] M. Saowadee, T. Lertwiriyaprapa, S. Chalermwisutkul, and P. Akkaraekthalin, "Novel approximate UTD ray solution for the radiation and scattering by antennas near a planar material junction on PEC ground plane," *Journal of Electromagnetic Waves and Applications*, vol. 31, no. 2, pp. 166–181, 2017.

[8] W. Burnside and K. Burgener, "High frequency scattering by a thin lossless dielectric slab," *IEEE Transactions on Antennas and Propagation*, vol. 31, no. 1, pp. 104–110, 1983.

[9] P. D. Holm, "A new heuristic UTD diffraction coefficient for nonperfectly conducting wedges," *IEEE Transactions on Antennas and Propagation*, vol. 48, no. 8, pp. 1211–1219, 2000.

[10] Y. I. Nechayev and C. C. Constantinou, "Improved heuristic diffraction coefficients for an impedance wedge at normal incidence," *IEE Proceedings - Microwaves, Antennas and Propagation*, vol. 153, no. 2, pp. 125–132, 2006.

[11] F. Sikta, W. Burnside, T.-T. Chu, and L. Peters, "First-order equivalent current and corner diffraction scattering from flat plate structures," *IEEE Transactions on Antennas and Propagation*, vol. 31, no. 4, pp. 584–589, 1983.

[12] M. Albani, F. Capolino, G. Carluccio, and S. Maci, "UTD vertex diffraction coefficient for the scattering by perfectly conducting faceted structures," *IEEE Transactions on Antennas and Propagation*, vol. 57, no. 12, pp. 3911–3925, 2009.

[13] P. J. Joseph, A. D. Tyson, and W. D. Burnside, "An absorber tip diffraction coefficient," *IEEE Transactions on Electromagnetic Compatibility*, vol. 36, no. 4, pp. 372–379, 1994.

[14] P. C. Chang, R. J. Burkholder, J. L. Volakis, R. J. Marhefka, and Y. Bayram, "High-frequency EM characterization of through-wall building imaging," *IEEE Transactions on Geoscience and Remote Sensing*, vol. 47, no. 5, pp. 1375–1387, 2009.

[15] D. Tami, C. G. Rego, D. Guevara et al., "Analysis of heuristic uniform theory of diffraction coefficients for electromagnetic scattering prediction," *International Journal of Antennas and Propagation*, vol. 2018, Article ID 3029152, 11 pages, 2018.

[16] A. Pimpatang and T. Lertwiriyaprapa, "Heuristic UTD corner and slope diffractions for antenna problem," in *2017 International Symposium on Antennas and Propagation (ISAP)*, Phuket, Thailand, October-November 2017.

[17] C. Mentzer, L. Peters, and R. Rudduck, "Slope diffraction and its application to horns," *IEEE Transactions on Antennas and Propagation*, vol. 23, no. 2, pp. 153–159, 1975.

[18] M. Saowadee, T. Lertwiriyaprapa, and S. Chalermwisutkul, "A preliminary study of a novel approximate UTD ray solution of an oblique EM diffraction by an impedance discontinuity in a planar surface," in *2013 10th International Conference on Electrical Engineering/Electronics, Computer, Telecommunications and Information Technology*, Krabi, Thailand, May 2013.